Electronic energy transfer in He*(2 ^1S)+Ne collisions: Propensity for odd-J levels of Ne*(5s,5s′,4d)

John Krenos
Department of Chemistry, Rutgers University, New Brunswick, New Jersey 08903
(Received 15 September 1983)

Electronic energy transfer in the He*(2 ^1S)+Ne system was studied in a nozzle-beam—scattering-cell experiment in which the visible emission of product Ne* was measured. Relative populations and cross sections of individual Ne* levels in the 5s, 5s′, and 4d manifolds were obtained at collision energies of 0.06 and 0.16 eV. The $3s_2$ Paschen level is the major product at both energies. In general, the formation of odd-J levels is favored and a qualitative explanation of this effect is proposed.

INTRODUCTION

It is well known that many lasing transitions of neon are enhanced by the presence of helium in the gaseous discharge. Only a general understanding of the discharge process is possible at this time; however, progress has been made in unraveling the dynamics of what may be the most important step, i.e., the transfer of electronic excitation from metastable helium atoms to neon by a bimolecular collision process.[1–6] Both triplet (2 ^3S) and singlet (2 ^1S) states of metastable helium are important energy carriers. The metastable energy levels are shown in Fig. 1 along with those of nearby electronic states of neon. Consider the He*(2 ^1S)+Ne reaction, which is the subject of this paper. One might expect that Ne* levels with small energy defects (such as the 5s,5s′ levels) should be favored channels as predicted by the time-honored propensity rule for collisions of the second kind. This has been demonstrated conclusively in single collision molecular-beam experiments.[1–3]

Siska and co-workers[1(a)] and Haberland and co-workers[2(a)–(d),(g)] have measured the angular and velocity distributions of metastable Ne* formed by radiative cascade from higher Ne* levels in crossed-beam He*(2 ^1S)+Ne experiments. Product Ne* levels were identified by kinematic constraints. The exoergic 5s levels (see Fig. 1) were only observed above the threshold energy for formation of the endoergic 5s′ levels. At still higher collision energy the 4d and 4f levels were seen; however, it was not possible to resolve individual states. In addition, Siska and co-workers[1(a),(c)] observed the very exoergic 3d′ levels above threshold for 5s′ formation. Both groups have modeled the energy-transfer process to some extent.[1(b)–(d),2(g)] A severe test of these models requires the energy-dependent cross section for formation of individual Ne* levels.

In a preliminary communication,[3] we reported relative cross sections for the 5s, 5s′ levels of Ne* at a collision energy of 0.06 eV. The collision energy spread in our room-temperature nozzle-beam—scattering-gas experiment was much greater than in the crossed-beam measurements. The visible fluorescence of Ne*, however, was resolved and level populations and their relative cross sections were obtained. In this paper we report relative level populations and cross sections for the formation of individual 5s, 5s′, and 4d levels of Ne* at 0.06 and 0.16 eV. Measurements are made with a cooled scattering cell (180 K) to reduce the collision energy spread. Our results are compared to the crossed-beam results[1,2] as well as to recent discharge flow[4] and total excitation transfer[6] measurements.

EXPERIMENTAL

The apparatus has been described in detail elsewhere.[7] The helium metastable beam is formed by electron impact (150-eV electrons) of a supersonic helium atom beam.

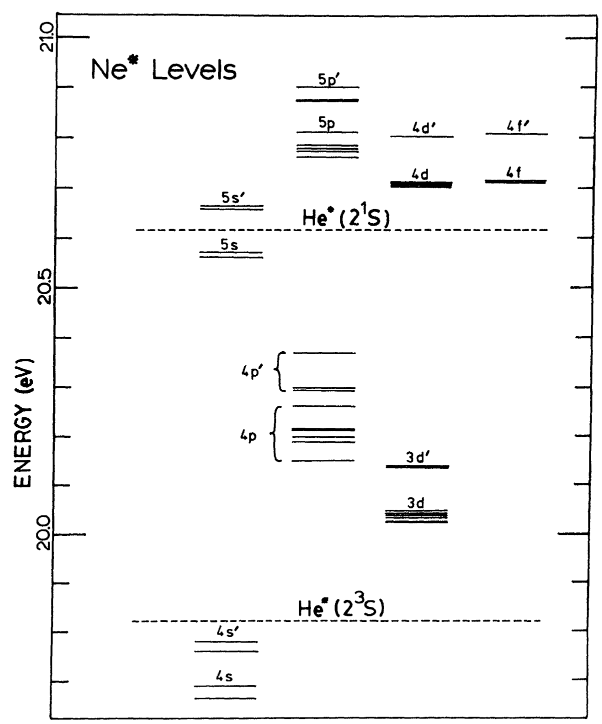

FIG. 1. Metastable energy levels of He and nearby levels of Ne.

The velocity distribution of the metastable beam is measured by the time-of-flight method. Neon pressure in the scattering cell is roughly 10^{-4} Torr. A room-temperature nozzle yields an average collision energy (relative kinetic energy in the center-of-mass system) of 0.06 eV, while a heated nozzle ($\sim$883 K) yields a value of 0.16 eV. When the nozzle and scattering cell are both at room temperature, the collision energy spread (full width at half maximum) is $\sim$0.07 eV. Experiments are also done at a scattering cell temperature of 180 K, which reduces the collision energy spread to $\sim$0.05 eV. The composition of the metastable beam is approximately 85% $2\,^1S$ and 15% $2\,^3S$ under our conditions.[1(a),8] The triplet component has insufficient energy to excite the $5s$, $5s'$, and $4d$ levels of Ne; however, at 0.16 eV the $3d$ levels are accessible in the high-energy tail of the $He^*(2\,^3S)+Ne$ collision energy distribution. Thus, we do not report $3d$ level populations at 0.16 eV.

Light emission in the scattering cell along the beam path is analyzed in the 300—870-nm spectral region by a 0.5-m scanning monochromator. Analyzed light emerging from the monochromator exit slit is focused onto the photocathode (Ga-As) of a cooled photomultiplier tube. A single-photon counting system is used to acquire and record spectra. The relative spectral response of the detection system is determined by a calibrated tungsten lamp. The neon emission spectrum was examined in low resolution (1.2-nm bandpass) over the entire wavelength region. The intense features of the spectrum were scanned at higher resolution sufficient to identify prominent lines and to separate cascade lines from direct transfer ones. The spectral region from 500—650 nm was studied with great care, since most of the visible lines emanating from the $5s$, $5s'$, and $4d$ levels are found there.

The best transitions for determining level populations in our experiment are given in Table I. The $3s_2$-$2p_4$ (632.8 nm) and $3s_4$-$2p_7$ (633.1 nm) transitions are resolved with great difficulty; thus they were not used in the population analysis. We use the transition probabilities of Lilly[9] (also given in Table I) to obtain steady-state level populations. The relative intensities of spectral lines originating from a common upper level are found to be in good agreement with those predicted from Lilly's transition probabilities. A more extensive test of Lilly's branching ratios was performed by Haak *et al.*,[10] who found good agreement as well.

Since all transitions from a given upper level are not observable in our experiments, we are not able to obtain the cross section by summation of line intensities. Instead, the steady-state populations are multiplied by total transition probabilities[9,11–13] given in Table II. Because these transition probabilities are obtained from several sources, the resulting relative cross sections are less certain than our level populations. Where possible, we use Lilly's values of transition probabilities, since they are used in our population analysis. The $3s_2$, $3s_4$, $4d_2$, and $4d_5$ levels are special cases in that they also radiate to the ground state of neon. For the $3s_2$ and $3s_4$ levels, we prefer the total transition probabilities obtained from the vacuum-uv lifetime measurements of Lawrence and Liszt.[11] For the $4d_2$ and $4d_5$ levels, we use the theoretical values of Gruzdev and Loginov.[12] For comparison, the values of Gruzdev and Loginov[12] are given in Table II for the other levels in the $3d$, $3d'$, $5s$, $5s'$, and $4d$ manifolds. Except for a few cases (e.g., $4d'_1$ and $4d_3$) their values are similar to the ones we have chosen.

TABLE I. Transitions used for population analysis.

Transition			
Paschen	Racah	Wavelength (nm)	$A(10^6\ s^{-1})$[a]
$4d'_1$-$2p_9$	$4d[\frac{5}{2}]^0_3$-$3p[\frac{5}{2}]_3$	574.83	2.76
$4d''_1$-$2p_8$	$4d[\frac{5}{2}]^0_2$-$3p[\frac{5}{2}]_2$	580.44	2.97
$4d_2$-$2p_8$	$4d[\frac{3}{2}]^0_1$-$3p[\frac{5}{2}]_2$	581.14	0.61
$4d_3$-$2p_{10}$	$4d[\frac{3}{2}]^0_2$-$3p[\frac{1}{2}]_1$	533.08	4.28
$4d_3$-$2p_9$	$4d[\frac{3}{2}]^0_2$-$3p[\frac{5}{2}]_3$	576.06	0.44
$4d_4$-$2p_8$	$4d[\frac{7}{2}]^0_3$-$3p[\frac{5}{2}]_2$	582.02	7.38
$4d'_4$-$2p_9$	$4d[\frac{7}{2}]^0_4$-$3p[\frac{5}{2}]_3$	576.44	9.51
$4d_5$-$2p_{10}$	$4d[\frac{1}{2}]^0_1$-$3p[\frac{1}{2}]_1$	534.11	6.24
$4d_5$-$2p_8$	$4d[\frac{1}{2}]^0_1$-$3p[\frac{5}{2}]_2$	582.89	0.25
$4d_6$-$2p_{10}$	$4d[\frac{1}{2}]^0_0$-$3p[\frac{1}{2}]_1$	534.33	7.84
$3s_2$-$2p_{10}$	$5s'[\frac{1}{2}]^0_1$-$3p[\frac{1}{2}]_1$	543.37	0.45
$3s_2$-$2p_7$	$5s'[\frac{1}{2}]^0_1$-$3p[\frac{3}{2}]_1$	604.61	0.20
$3s_2$-$2p_6$	$5s'[\frac{1}{2}]^0_1$-$3p[\frac{3}{2}]_2$	611.80	0.64
$3s_3$-$2p_5$	$5s'[\frac{1}{2}]^0_0$-$3p'[\frac{3}{2}]_1$	631.37	3.3
$3s_4$-$2p_{10}$	$5s[\frac{3}{2}]^0_1$-$3p[\frac{1}{2}]_1$	566.25	0.51
$3s_4$-$2p_8$	$5s[\frac{3}{2}]^0_1$-$3p[\frac{5}{2}]_2$	621.39	2.7
$3s_5$-$2p_{10}$	$5s[\frac{3}{2}]^0_2$-$3p[\frac{1}{2}]_1$	568.98	1.3
$3s_5$-$2p_9$	$5s[\frac{3}{2}]^0_2$-$3p[\frac{5}{2}]_3$	618.21	3.6
$3s_5$-$2p_6$	$5s[\frac{3}{2}]^0_2$-$3p[\frac{3}{2}]_2$	644.47	1.14
$3s_1'''$-$2p_4$	$3d'[\frac{5}{2}]^0_3$-$3p'[\frac{3}{2}]_2$	865.44	38.30
$3d_4$-$2p_8$	$3d[\frac{7}{2}]^0_3$-$3p[\frac{5}{2}]_2$	849.54	37.95
$3d'_4$-$2p_9$	$3d[\frac{7}{2}]^0_4$-$3p[\frac{5}{2}]_3$	837.76	49.23

[a]Transition probabilities for $5s,5s'$ levels from Ref. 9(a); $3d,3d'$ from Ref. 9(b); $4d$ from Ref. 9(c).

Since the $3s_2$, $3s_4$, $4d_2$, and $4d_5$ levels also radiate to the ground state of neon, we must assess the effect of self-absorption on our observed level populations. The effect should be most pronounced on the vacuum-uv lines, which we do not measure. The intensity of the visible lines originating from the $3s_2$, $3s_4$, $4d_2$, and $4d_5$ levels will be increased by uv self-absorption followed by visible reradiation to some extent. Since only light emitted along the beam axis is collected efficiently, we can ignore reradiation effects occurring outside this small region. A simple calculation along the lines of Mitchell and Zemansky[14] for a neon number density of 3×10^{12} atoms cm^{-3} (10^{-4} Torr), a path length of 0.1 cm (the radius of the cylindrical collision zone), and a thermal Doppler profile predicts a maximum increase in the visible region $3s_2$, $3s_4$, $4d_2$, and $4d_5$ line intensities of $\sim$1% relative to spectral

TABLE II. Total transition probabilities for Ne* levels.

Level (Paschen)	A_{total} (10^6 s^{-1})[a]	Reference(s)
$4d_1'$	14.9 (19.3)	9(c),13
$4d_1''$	14.9 (14.8)	9(c),13
$4d_2$	56.5	12
$4d_3$	16.4 (28.2)	9(c),13
$4d_4$	15.3 (13.3)	9(c),13
$4d_4'$	16.1 (18.6)	9(c),13
$4d_5$	27.0	12
$4d_6$	17.8 (21.5)	9(c),13
$3s_2$	43.3 (45.0)	11
$3s_3$	13.0 (10.3)	9(a)
$3s_4$	51.3 (54.9)	11
$3s_5$	13.0[b] (13.4)	9(a)
$3s_1'''$	46.1 (62.1)	9(b)
$3d_4$	46.4 (37.7)	9(b)
$3d_4'$	49.2 (54.1)	9(b)

[a]Values in parentheses from Ref. 12.
[b]$3s_5$-$2p_5$ transition probability corrected to 0.065 in Ref. 9(a).

lines from levels not radiatively coupled to the ground state. This increase is too small to measure in our system. Indeed, within a neon pressure range between 10^{-5} and 10^{-3} Torr, the relative line intensities do not vary.

RESULTS

Emission from the 5*s*, 5*s*′, and 4*d* levels of Ne* is seen at both 0.06 and 0.16 eV. Integrated line intensities corrected for spectral response are divided by appropriate transition probabilities (see Table I) to obtain steady-state level populations, which are reported in Table III. Lines originating from the $3s_2$, $3s_5$, $4d_4$, and $4d_4'$ levels are resolved neatly, so the random error in the relative populations is limited only by photon counting statistics. The error is larger for the other levels, since their emission lines are not resolved as cleanly. Level populations are independent of scattering-cell temperature except for the 4*d* levels at 0.06 eV, which are formed by the high-energy tail of the collision energy distribution. Cooling the scattering cell narrows the distribution and concomitantly lowers the population of the 4*d* levels relative to 5*s* and 5*s*′. The level energies are given in Table III relative to He*($2\,^1S$). At 0.16 eV, all the levels in Table III are "energetically" open to most of the He*+Ne colliding pairs at both scattering cell temperatures and no significant variation in relative level populations is observed.

Our room-temperature nozzle—scattering-cell results are compared to level populations obtained in a discharge flow apparatus[4] in Table III. In general, agreement is surprisingly good considering that in the flow system: (1) post-reaction collisions of Ne* with He could modify nascent level populations; (2) the collision energy distribution is likely to be quite different; and (3) other energy carriers are present [such as He*($2\,^1P$)], which persist because of radiation trapping. A major disagreement is seen, howev-

TABLE III. Ne* relative populations.

Level (Paschen)	Energy (meV)[a]	Populations[b]			Ref. 4
$4d_1'$	95.9		<3	13	4.6
$4d_1''$	95.7		<3	13	3.2
$4d_2$	93.2		<3	10	2.5
$4d_3$	91.3	<1	5	15	4.3
$4d_4$	90.0	10±3	18±4	30±5	6.7
$4d_4'$	89.8	5±1	9±2	10±2	8.4
$4d_5$	86.8	[c]	5	7	3.2
$4d_6$	85.8	[c]	2	3	0.9
$3s_2$[d]	47.2	100	100	100	100
$3s_3$	41.0	<3	<2	<4	0.5
$3s_4$	−45.0	18±8	18±8	10±4	11
$3s_5$	−55.5	21±4	20±4	13±2	10
T (nozzle)		298 K	298 K	883 K	
T (scattering cell)		180 K	298 K	298 K[e]	<390 K
$\langle E \rangle$ (meV)		58	60	160	<50

[a]Level energy relative to He*($2\,^1S$).
[b]Standard deviation ±50% unless otherwise noted.
[c]Combined population ($4d_5+4d_6$)∼4.
[d]$3s_2$ level population normalized to 100.
[e]Similar result for 180 K.

er, in the relative populations of the $4d_4$ and $4d'_4$ levels, which form a multiplet pair with Racah designations of $4d(\frac{7}{2})^0_3$ and $4d(\frac{7}{2})^0_4$, respectively. The level separation is only 1.1 cm^{-1} and we see a greater population of the higher energy $4d_4$ level with respect to $4d'_4$. The flow experiment gives the opposite result. It appears likely that the flow population of $4d'_4$ is enhanced by secondary collisions of $Ne^*(4d_4)$ with He, resulting in depopulation of the $4d_4$ level. Intramultiplet energy-transfer rate constants can be quite large (up to 3×10^{-10} cm^3 $molecule^{-1}\,s^{-1}$) as shown by Chang *et al.*[15] for Kr* in Ar. A rate constant of 3×10^{-10} $cm^3\,molecule^{-1}\,s^{-1}$ for $4d_4\rightarrow4d'_4$ conversion is sufficient to provide a collisional relaxation pathway competing favorably with radiative processes at the helium pressure used by Haak *et al.*[4]

As discussed previously, all transitions from a given upper level are not observable in our experiments and we are not able to obtain level cross sections by summation of line intensities. Instead, the steady-state populations in Table III are multiplied by total transition probabilities given in Table II. The resulting relative cross sections are given in Table IV. Two important results are immediately evident. The total $5s$, $5s'$ cross section is greater than the total $4d$ cross section at both collision energies and the total cross section for production of odd-J levels surpasses the total for even-J levels. The propensity for odd-J levels in the $5s,5s',4d$ manifolds will be treated in the discussion section. Our $4d$ to $5s,5s'$ cross section ratio has interesting consequences when combined with the results of Haberland *et al.*[2(g)]

Haberland, Konz, and Oesterlin[2(g)] calculated total scattering and energy-transfer cross sections for $He^*(2\,^1S)+Ne$ by using potential curves and coupling matrix elements derived from simultaneous fits of measured elastic and inelastic differential cross sections. The He-Ne* curves were slightly modified He-Ne^+ curves of Dabrowski and Herzberg.[16] The $4d,4f$ levels were treated as a group, so no direct comparison with our individual level cross sections is possible. They do report the cross section ratio for the combined $4d,4f$ levels versus the single $3s_2$ level to be 2.2 at 0.174 eV, which is an energy close to our 0.16-eV experiment. Our total $4d$ vs $3s_2$ cross section ratio is 0.48 at 0.16 eV. By combining the different experimental results, we obtain a prediction for the total $4f$ vs $3s_2$ cross section ratio to be 1.7 near 0.16 eV. This also implies that the $4f$ levels are favored by a factor of 3.5 over the $4d$ levels. These results are difficult to explain. Feltgen and co-workers[6] have measured total excitation cross sections directly from Ne* vacuum-uv emission as a function of collision energy. A much smaller total $4d/4f$ cross section than reported by Haberland *et al.*[2(g)] is required to explain their data. It appears that a direct measurement of $4f$ cross sections is necessary to resolve the conflicting results. It is interesting that Feltgen and co-workers[6] also report $3s_4,3s_5$ excitation with cross sections about 10—20% of the $3s_2$ cross section at threshold. This is in good agreement with our results (see Table IV) considering the large uncertainty in our $3s_4$ value.

Since there is evidence for $3d$ level product formation in other studies,[1(a),1(c),4] we also looked for and found $3d$ emissions. Unfortunately, they are in an unfavorable spectral region, so only a rough estimate of relative population is possible (see Table V). The cascade contribution is estimated from our $5s$, $5s'$, and $4d$ level populations and appropriate transition probabilities.[9,11,12] There appears to be excess population attributable to direct reaction. In Table V, we report relative cross sections for the $3s'''_1$, $3d_4$, and $3d'_4$ levels at 0.06 eV, derived from the excess population. Total populations are in good agreement with the discharge flow measurement,[4] but inversion of $3d_4$, $3d'_4$ population is seen similar to what is found for $4d_4$, $4d'_4$ (see Table III).

TABLE IV. Ne* relative cross sections.

Level (Paschen)	J	Cross sections[a]		
$4d'_1$	3		<1	4.5
$4d''_1$	2		<1	4.5
$4d_2$	1		<4	13
$4d_3$	2	<0.4	2	6
$4d_4$	3	3.5±1.0	6.4±1.4	11±2
$4d'_4$	4	1.9±0.4	3.3±0.7	3.7±0.7
$4d_5$	1	b	3	4
$4d_6$	0	b	1	1
$3s_2^c$	1	100	100	100
$3s_3$	0	<1	<1	<1
$3s_4$	1	21±10	21±10	12±5
$3s_5$	2	6.3±1.2	6.0±1.2	3.9±0.6
$\langle E\rangle$ (meV)		58	60	160

[a]Standard deviation ±50% unless otherwise noted.
[b]Combined cross section $(4d_5+4d_6)\sim2$.
[c]$3s_2$ level cross section normalized to 100.

DISCUSSION

The most dramatic observation we have made is the propensity for odd-J levels in the $5s,5s',4d$ manifolds of Ne excited by $He^*(2\,^1S)$. In the jl-coupling scheme, the total electronic angular momentum of the Ne* core $(j=\frac{3}{2},\frac{1}{2})$ couples with the orbital angular momentum (l) of the Rydberg electron to produce a resultant angular momentum that has half-integer quantum numbers. The jl levels are then split into doublets by the spin of the

TABLE V. Populations and cross sections of certain $3d,3d'$ levels.[a]

Level (Paschen)	Total population Ref. 4	Total population This work	Excess[b]	Cross section[c]
$3s'''_1$	3.6	3.5	2.1	2.2
$3d_4$	2.8	2.4	1.6	1.7
$3d'_4$	3.2	1.1	0.6	0.7

[a]Relative to $3s_2$ normalized to 100.
[b]Our population after cascade correction.
[c]Cross section based on our excess population.

Rydberg electron. Each doublet contains one level of odd and one level of even J. In the $He^*(2\,^1S)+Ne$ reaction, formation of the odd-J member of the doublet is favored over the even one for the $5s,5s',4d$ levels. An apparent exception is the $4d'_1,4d''_1$ doublet at 0.16 eV (see Table IV). Unfortunately, the error in our measurement ($\pm50\%$) is significantly large and a better experiment is required to determine whether there actually is an exception here.

The dynamics of energy transfer is most easily visualized in terms of potential-energy curves and their crossings. The entrance channel, $He^*(2\,^1S)+Ne$, has a diabatic potential energy curve ($^1\Sigma^+$), which has been determined by theory[1(d),17] and experiment.[1(c),2(g)] The curve is repulsive in character and possesses a weak long-range van der Waals minimum. Siska[1(d)] has calculated $^1\Sigma^+$ potential-energy curves for $He+Ne^*$ exit channels using a one-electron model potential method. Some of the curves look very much like weakly perturbed $He+Ne^+$ curves,[16] while others appear strongly perturbed and exhibit avoided crossings [see Fig. 5 of Ref. 1(d)]. The He^*+Ne curve first crosses a curve correlating with $Ne^*(3s_2)$ product at $\sim$3.2 Å, and then it crosses other curves at smaller values of the internuclear distance. The crossing at 3.2 Å is a dominant factor in the collision dynamics, since the $Ne^*(3s_2)$ level is the major product at both 0.06 and 0.16 eV. There are other curve crossings that account for the formation of the $3d_4$, $3s_1''''$, $3s_4$, $4d_5$, and $4d_4$, levels of Ne^* in the Siska model. We need to understand the origin of the other channels we observe and the propensity for odd-J levels in general.

To explain the preference for $5s$, $5s'$, and $4d$ levels of Ne^* with odd J, we adopt a Hund's case (c) approach, which is often appropriate for Rydberg-state molecules. The He^*+Ne potential-energy curve is of the $\Omega=0^+$ type and transitions to electronic states of $He+Ne^*$ could occur by a radial coupling mechanism,[18] which couples states of the same Ω. Odd-J levels of Ne^* form $\Omega=0^+$ states with ground-state He, if the l quantum number of the Rydberg electron of Ne^* is even. This is the case for the $5s$, $5s'$, and $4d$ manifolds of Ne^*, and a pathway for the formation of all odd-J levels in these manifolds exists provided suitable curve crossings are accessible during a collision.

If electronic parity conservation were unimportant, then even-J levels, which all produce $\Omega=0^-$ molecular states with ground-state He, could also be formed by the radial coupling mechanism. The $3s_3$ and $4d_6$ levels of Ne^* have $J=0$; thus only $\Omega=0^-$ molecular states are produced and a test of parity conservation is possible. The cross section for these two levels is very small (see Table IV); therefore, direct or indirect coupling of 0^+ and 0^- states is weak and changes in electronic parity are not facile. The even-J levels with $J\neq0$ must be produced by a mechanism allowing for changes in Ω, such as angular coupling.[18] Odd-J levels may also be formed by an angular coupling mechanism, but the primacy of the odd-J levels suggests that radial coupling is the dominant process. The role of the various coupling mechanisms requires further experimental and theoretical testing.

CONCLUSIONS

The electronic energy-transfer reaction

$$He^*(2\,^1S)+Ne\rightarrow He+Ne^*(5s,5s',4d)$$

exhibits propensity for formation of odd-J levels of Ne^*. This can be explained by a curve-crossing mechanism, in which $\Omega=0^+$ entrance and exit channel molecular states of $(HeNe)^*$ are coupled directly or indirectly through intermediate states. The coupling process is of the radial type. The even-J levels presumably arise from angular (rotational) coupling between molecular states of different Ω. This is a less important process. Levels with $J=0$ form 0^- molecular states with He and these levels have small cross sections. This argues for the importance of electronic parity conservation in the collision process.

ACKNOWLEDGMENTS

Financial support from the Research Council of Rutgers University and the Research Corporation is gratefully acknowledged. This work has benefited from correspondence and/or conversations with Professor P. Siska and Dr. H. Haberland, Dr. P. Oesterlin, and Dr. R. Feltgen. The assistance of Professor J. Bel Bruno proved invaluable. This paper was written during a sabbatical year at the Massachusetts Institute of Technology (MIT). Useful discussions with Professor J. Kinsey and Professor R. Field, Dr. H. L. Dai, Mr. D. Imre, and Mr. A. Sinha are acknowledged as well as the hospitality of all the MIT physical chemists.

---

[1](a) D. W. Martin, T. Fukuyama, R. W. Gregor, R. M. Jordan, and P. E. Siska, J. Chem. Phys. 65, 3720 (1976); (b) P. E. Siska and T. Fukuyama, in *Abstracts of the Tenth International Conference on the Physics of Electronic and Atomic Collisions, Paris, 1977,* edited by M. Barat and J. Reinhardt (Commissariat à L'Energie Atomique, Paris, 1977), p. 552; (c) T. Fukuyama and P. E. Siska, in *Abstracts of the Eleventh International Conference on the Physics of Electronic and Atomic Collisions, Kyoto, 1979,* edited by K. Takayanagi and N. Oda (The Society for Atomic Collisions Research, Kyoto, 1979), p. 460; (d) P. E. Siska, J. Chem. Phys. 73, 2372 (1980).

[2](a) H. Haberland, P. Oesterlin, and K. Schmidt, J. Chem. Phys. 65, 3373 (1976); (b) P. Oesterlin, H. Haberland, and K. Schmidt, in Ref. 1(b), p. 558; (c) H. Haberland and P. Oesterlin, in *Abstracts of the Seventh International Symposium on Molecular Beams, Trento, Italy, 1979,* edited by G. Scoles (Libera Universitàdi Trento, Trento, 1979), p. 78; (d) H. Haberland and P. Oesterlin, in Ref. 1(c), p. 458; (e) H. Haberland, in

Abstracts of the Twelfth International Conference on the Physics of Electronics and Atomic Collisions, Gatlinburg, 1981, edited by S. Datz (North-Holland, Amsterdam, 1982), p. 520; (f) H. Haberland and P. Oesterlin, Z. Phys. A 304, 11 (1982); (g) H. Haberland, W. Konz, and P. Oesterlin, J. Phys. B 15, 2969 (1982).

[3]J. Krenos, in Ref. 2(c), p. 75.

[4]H. K. Haak, B. Wittig, and F. Stuhl, Z. Naturforsch. 35a, 1342 (1980).

[5](a) A. L. Schmeltekopf and F. C. Fehsenfeld, J. Chem. Phys. 53, 3173 (1970); (b) W. Lindinger, A. L. Schmeltekopf, and F. C. Fehsenfeld, J. Chem. Phys. 61, 2890 (1974); (c) D. W. Ernie and H. J. Oskam, Phys. Rev. A 21, 95 (1980).

[6]R. Feltgen and co-workers (private communication).

[7](a) J. Krenos and J. Bel Bruno, Chem. Phys. Lett. 49, 447 (1977); (b) J. Bel Bruno, Ph.D. thesis, Rutgers University, 1980.

[8]C. H. Chen, H. Haberland, and Y. T. Lee, J. Chem. Phys. 61, 3095 (1974).

[9](a) R. A. Lilly, J. Opt. Soc. Am. 65, 389 (1975); (b) 66, 245 (1976); (c) 66, 971 (1976).

[10]H. K. Haak, C. Zetsch, and F. Stuhl, Z. Naturforsch. 35a, 1337 (1980).

[11]G. M. Lawrence and H. S. Liszt, Phys. Rev. 178, 122 (1969).

[12]P. F. Gruzdev and A. V. Loginov, Opt. Spektrosk. 35, 3 (1973).

[13]P. W. Murphy, J. Opt. Soc. Am. 58, 1200 (1968).

[14]A. C. G. Mitchell and M. W. Zemansky, *Resonance Radiation and Excited Atoms* (Cambridge University, Cambridge, 1971), pp. 92—106.

[15]R. S. F. Chang, H. Horiguchi, and D. W. Setser, J. Chem. Phys. 73, 778 (1980).

[16]I. Dabrowski and G. Herzberg, J. Mol. Spectrosc. 73, 183 (1978).

[17]G. Peach, J. Phys. B 11, 2107 (1978).

[18]For a discussion of radial and angular coupling mechanisms, see R. W. Anderson, J. Chem. Phys. 77, 5426 (1982), and references cited therein.